NASA Environmentally Responsible Aviation High Overall Pressure Ratio Compressor Research – Pre-Test CFD

Mark L. Celestina[1]
John C. Fabian[2]
Sameer Kulkarni[3]
NASA Glenn Research Center, Cleveland, Ohio, 44135

This paper describes a collaborative and cost-shared approach to reducing fuel burn under the NASA Environmentally Responsible Aviation project. NASA and General Electric (GE) Aviation are working together as an integrated team to obtain compressor aerodynamic data that is mutually beneficial to both NASA and GE Aviation. The objective of the High OPR Compressor Task is to test a single stage then two stages of an advanced GE core compressor using state-of-the-art research instrumentation to investigate the loss mechanisms and interaction effects of embedded transonic highly-loaded compressor stages. This paper presents preliminary results from NASA's in-house multistage computational code, APNASA, in preparation for this advanced transonic compressor rig test.

Nomenclature

Nc	=	Wheel Speed
OPR	=	Overall Pressure Ratio
PRN	=	Normalized Pressure Ratio (normalized by Data Match)
TRN	=	Normalized Temperature Ratio (normalized by Data Match)

I. Introduction

THE Propulsion Technology Sub-element of the Environmentally Responsible Aviation (ERA) Project has a stated goal of reducing fuel burn. This goal can be achieved by increasing the overall pressure ratio (OPR) of the compression system and thus increasing the thermal efficiency of aircraft propulsion systems. The ERA Project under the Integrated System Research Program (ISRP) has embarked on a collaborative and cost-shared approach to advancing these goals. NASA and General Electric (GE) Aviation are working together as an integrated team to meet critical NASA and GE project milestones. The team has selected an advanced GE core compressor to test. The objective of this test is to obtain front block core compressor aerodynamic data that is mutually beneficial to both NASA and GE Aviation. Using this approach, the High OPR Compressor Task's objective is to test the first two stages of an embedded GE core compressor using state-of-the-art research instrumentation to investigate the loss mechanisms and interaction effects of highly-loaded compressor stages. The objective of this paper is to present pre-test results in preparation of the test to better understand the complex flow physics for this advanced transonic compressor rig using NASA's in-house multistage computational code, APNASA.

II. W7 Multistage Compressor Facility

The W7 multistage compressor test facility in the Engine Research Building (ERB) at NASA Glenn Research Center will be used to run this test. This facility is capable of running up to 18,756 RPM in both directions and a goal was set to accurately measure mass flow to within 0.7%. The massflow range of this facility varies from 10 to 100 lbm/sec. The massflow accuracy capability was a result of modernizing the facility by upgrading mitered elbows and replacing the flow metering system. Due to the limited L/D runs of the inlet piping, the orifice plate flow meter system was replaced with a Mc Crometer V-Cone meter system that is widely accepted in the natural gas pipeline and process gas industries. The V-cone was calibrated to reduce the discharge coefficient uncertainty to a low level. Other improvements include replacing the mitered elbows with long radius elbows. To lessen the impact of swirl from the long radius elbows, a Cheng Rotation Vane (CRV) was installed upstream of the first long radius

[1] Task Lead, Turbomachinery & Heat Transfer Branch, 21000 Brookpark Rd./Mail Stop 5-9.
[2] Tech Lead, Turbomachinery & Heat Transfer Branch, 21000 Brookpark Rd./Mail Stop 5-10.
[3] Aerospace Engineer, Turbomachinery & Heat Transfer Branch, 21000 Brookpark Rd./Mail Stop 5-10.

elbow. Three differential pressure transducers will be connected in series to further reduce the mass flow uncertainty. Figure 1 shows a sketch of the updated facility.

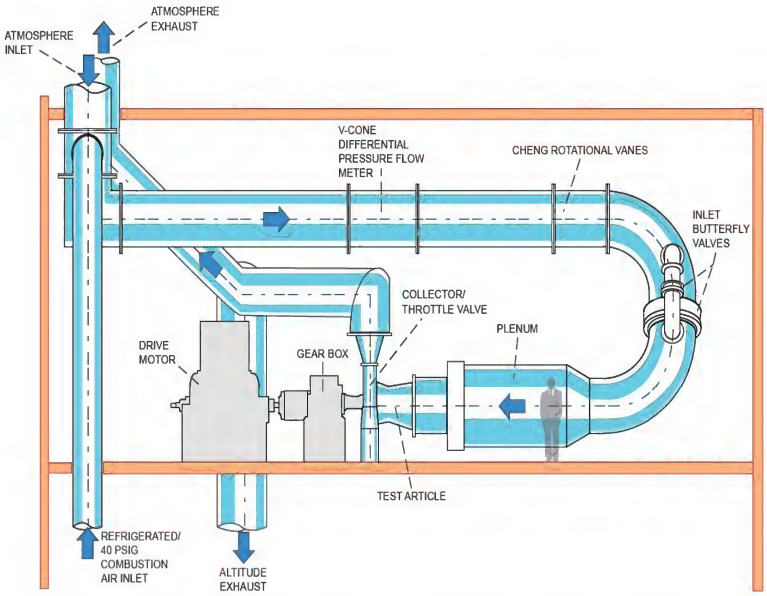

Figure 1. Rendering of the W7 multistage compressor facility.

III. GE Compressor Test Article

The test hardware has two configurations which share a common upstream flowpath consisting of a gooseneck, strut, and variable inlet guide vane (IGV). In the first configuration, shown in Figure 2, the downstream flowpath consists of a single stage downstream of the IGV. The second configuration is shown in Figure 3 and contains an additional stage behind the first configuration stage. Both the IGV and stators 1 and 2 are variable. The test objective is to determine the loss mechanisms and interaction effects of an embedded transonic stage. This will be accomplished by running the rig as a first stage only test and then adding the second stage to test the two stage configuration. The test objective of these two configurations is to determine the location and mechanism of loss. Since this is the front block of a compressor, it is thought that the spilled bow shock from rotor 2 will interact with the upstream stator 1 flow field. This complex inter-blade row interaction phenomenon has been hypothesized to be a cause of inaccuracy in prior mixing plane calculations.

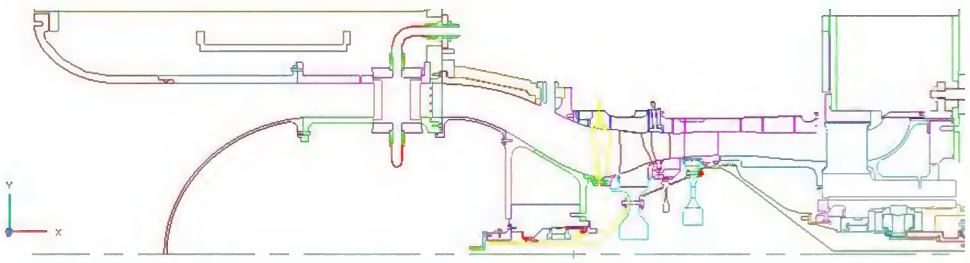

Figure 2. First configuration consists of a single stage.

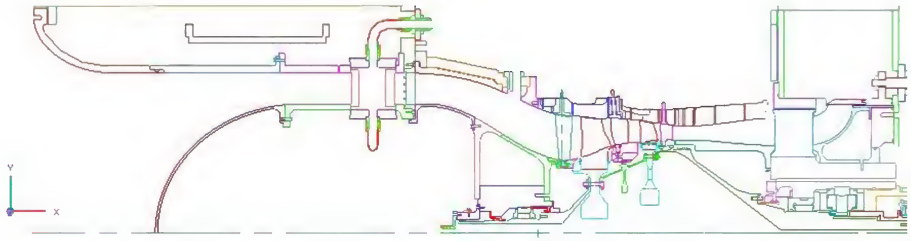

Figure 3. Second Configuration consists of two stages.

IV. Code Description

The analysis code used in this study solves the Average-Passage equation system (see Adamcyk[1] and Adamczyk, et. al.[2]). The equations are discretized using a finite volume formulation and are converged to steady-state using a 4-stage Runge-Kutta scheme employing the standard convergence accelerants such as local time-stepping and implicit residual smoothing. Details of the code can be found in Adamczyk, et. al.[3]. Flow in the clearance gaps is simulated using a model suggested by Kirtley, et. al.[4] which treats the flow through the clearance gap as an orifice flow with no loss in mass, momentum or energy. The same model is used to simulate clearance through the gap of the variable IGV and stator. The effect of the vena contracta which occurs in orifice flows is accounted for by the use of a discharge coefficient, which sizes the effective tip gap to the actual clearance. A discharge coefficient of 1.0 is used for all results presented herein as advocated by VanZante, et. al.[5]. The turbulence model used in this work is the standard k-ε two equation model found in Shabbir, et. al.[6].

V. Mesh Description

The flowpath of the first configuration test rig is shown in Figure 4. The APNASA system requires a unique local mesh for each of the four blade rows of the test rig which share a common axisymmetric global mesh as shown in Table 1. The computational grids used for the present calculations were generated using TGS developed by Beach[7]. The grids used by APNASA are sheared H-type in the blade-to-blade direction and incorporate a hyperbolic stretching parameter to resolve the boundary layer and adequately define the core flow region. The same stretching parameter is also used in the span-wise and chord-wise directions to enable adequate resolution of the blade leading and trailing edges and clearance gaps. The blade-to-blade stretching is relaxed to uniform spacing upstream and downstream of the blade rows since the flow is assumed to be periodic in those regions.

Table 1. Mesh Information for Configuration 1.

Configuration 1 Mesh	Extent	Axial Cells in Domain	Axial Cells within Blade Passage	Radial Cells	Circumferential Cells	Total Cells
Axisymmetric	Global	536	60	64		34,304
Strut	Local	220	60	64	50	704,000
IGV	Local	222	60	64	50	710,400
Rotor 1	Local	194	60	64	50	620,800
Stator 1	Local	214	60	64	50	684,800

The global axisymmetric mesh is shown in Figure 4 and illustrates the clustering of points near the leading and trailing edges of each blade row for the first configuration. The blade rows have been labeled for clarification. The extent of three-dimensional local meshes run from mid-chord of the upstream blade row to mid-chord of the downstream blade row. This rule has been developed over a number of validation exercises of many different compressor and turbine geometries and has been found to capture the upstream and downstream influences of the smeared out blade rows on the blade row of interest. This rule is excepted for the first and last blade rows of the domain which extend to the inlet and exit planes, respectively. There is no mixing plane interface between blade rows in the APNASA system. The influence of upstream and downstream blade rows on the blade row of interest are represented by body forces and energy source terms which arise from imposing the constraint of a unique axisymmetric solution on the system.

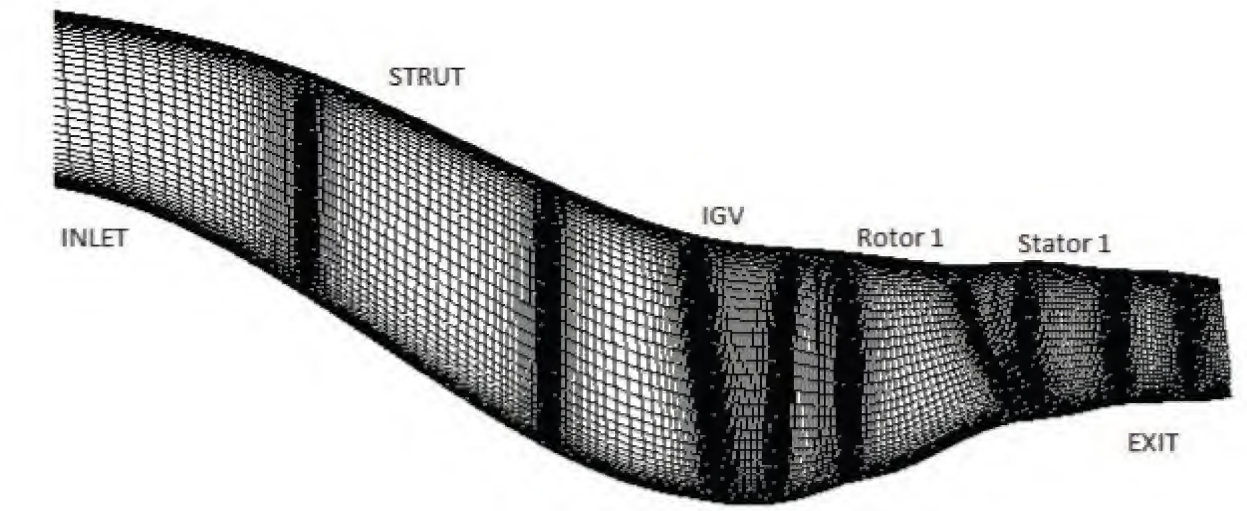

Figure 4. Global Axisymmetric Mesh for Configuration 1.

The flowpath of the second configuration is shown in Figure 5. The axisymmetric mesh for the second configuration extends further than the first configuration to accommodate the additional stage. The grid sizes are presented in

Table **2**. Note the difference between the two configuration meshes is the meshes for the second stage. The first configuration mesh is simply a truncation of the second configuration mesh.

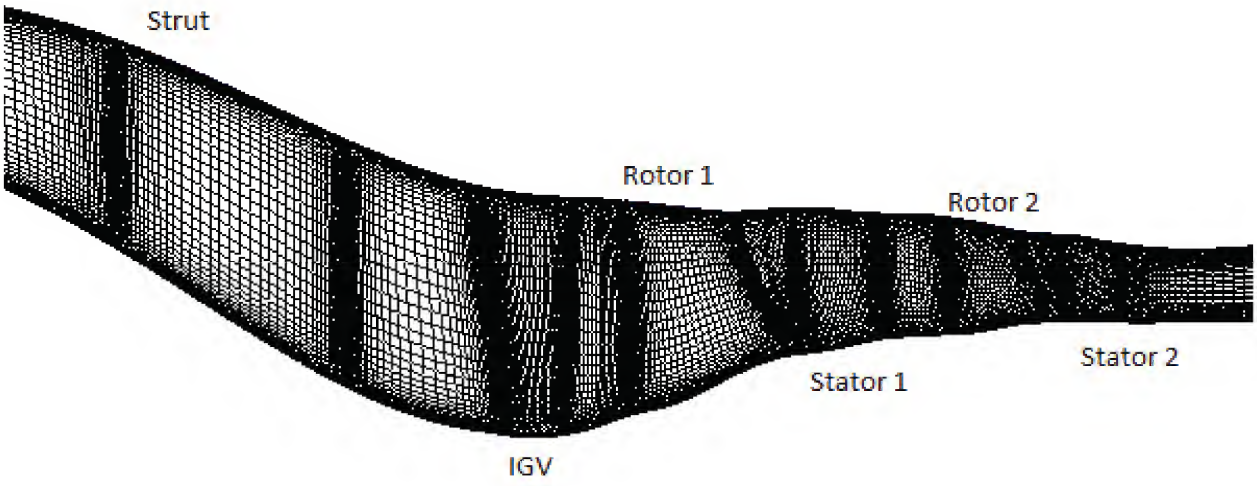

Figure 5. Global Axisymmetric Mesh for Configuration 2.

Table 2. Mesh Information for the Second Configuration.

Configuration 2 Mesh	Extent	Axial Cells in Domain	Axial Cells within Blade Passage	Radial Cells	Circumferential Cells	Total Cells
Axisymmetric	Global	729	60	64		46,656
Strut	Local	220	60	64	50	704,000
IGV	Local	222	60	64	50	710,400
Rotor 1	Local	194	60	64	50	620,800
Stator 1	Local	214	60	64	50	684,800
Rotor 2	Local	214	60	64	50	684,800
Stator 2	Local	197	60	64	50	630,400

VI. Results

The first configuration consisting of an IGV and single stage with upstream strut was run at 97% Nc. The simulation was run with clearance over Rotor 1 and the setting angles for the IGV, Stators 1 and 2 consistent with those from a proprietary quasi three-dimensional code with data match called CAFMIX. The CAFMIX result is a throughflow code solution run to match previous test data. It was also assumed that there was a small amount of flow entering the computational domain in the gap between the rotor and stator and an equal amount egressing from the domain aft of the stator due to the under-platform cavity. The IGV and Stator 1 are variable thus a small clearance gap was assumed to exist from 50% chord to the trailing edge. Results for the computationally generated speedline are given in Figure 6. The figure presents a speedline of two integrated quantities, one of normalized Pressure Ratio (PR) and the other of normalized Temperature Ratio (TR) vs. normalized corrected mass flow. The quantities have been normalized by the value of the data match. The values used in the numerical speedline are computed by integrating the mass-averaged total pressure and total temperature at a mesh plane upstream of the IGV leading edge but downstream of the strut and a mesh plane downstream of the stator 1 trailing edge. The left-most point on the numerical speedline was not carried to stall. The normalized pressure ratio from the numerical speedline overpredicts the data match and indicates that the correct loss level or blockage has not been captured in the numerical simulation. The normalized temperature ratio, however, underpredicts the data match which suggests that the work input is underpredicted. With the PR overpredicted and the TR underpredicted, the difference in adiabatic efficiency as computed from the integrated PR and TR between the numerical simulation and the data match is large, on the order of 6 percent.

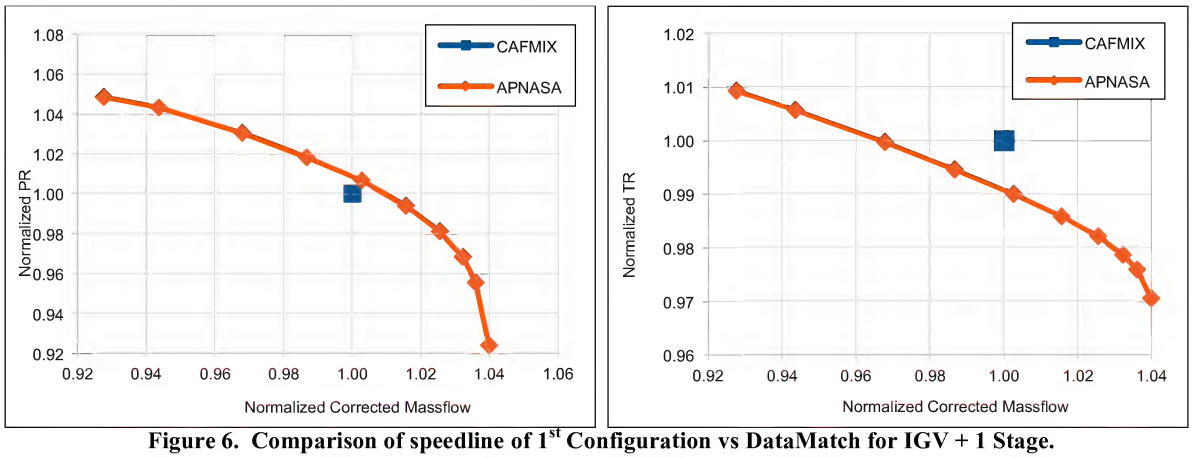

Figure 6. Comparison of speedline of 1st Configuration vs DataMatch for IGV + 1 Stage.

A numerical speedline was generated for the second configuration and is shown in Figure 7. The geometry was run under the same conditions described earlier for configuration 1. The normalized pressure and temperature ratio shown is the integrated quantities measured from a plane upstream of the IGV leading edge to a plane downstream of the second stage. The numerical speedline overpredicts the data match pressure ratio which again indicates that the loss level or blockage is underpredicted. Similarly, the Temperature Ratio from the numerical speedline underpredicts the data match. Interestingly, the speedline for the 2nd configuration was not able to achieve the normalized corrected massflow of the data match. Upon investigation of the numerical solution of the 2nd configuration, it was found that there was a strong oblique bow shock upstream of the 2nd rotor in the numerical simulation indicating that it was not started. This condition persisted in all four of the points on the numerical speedline. A numerical solution at a lower normalized mass flow was not attainable. A similar result was found by Adamczyk, et. al.[8] in which a small highly aggressive two stage machine was designed, fabricated and tested under the Advanced Small Turboshaft Compressor (ASTC) Program. He found that the 2nd rotor of the original design did not start at its design conditions resulting in a large drop in efficiency. The remedy to this situation was to decrease the massflow upstream of rotor 2 by either reducing the throat area or increasing the blockage through the first stage. In the present case, there is a mismatch between the stages due to the fact that the first stage is too efficient which is reducing the corrected flow into the 2nd stage and increasing its corrected speed. This tends to push the second stage to its unstarted characteristic. Thus the unstart is a result of the wrong efficiency and probably not the cause of it.

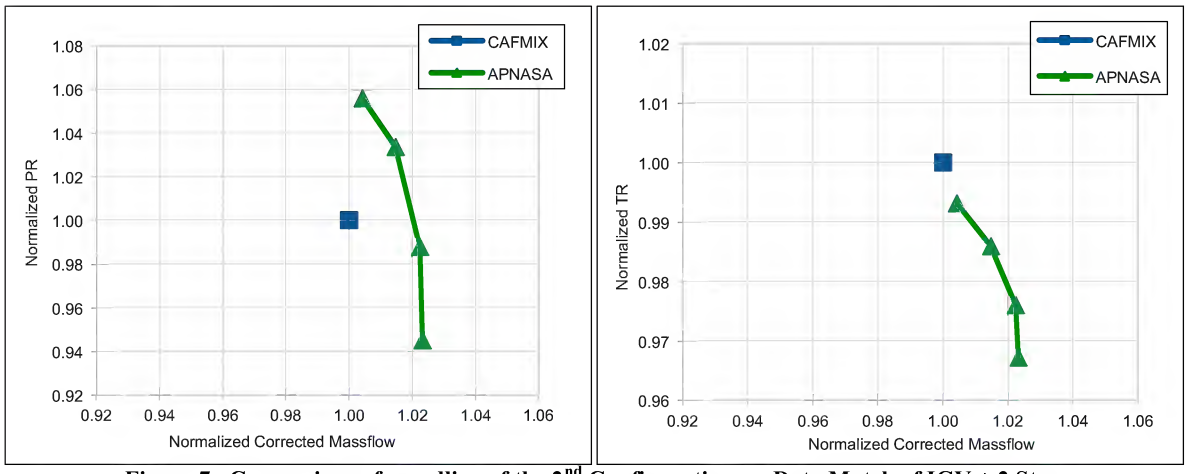

Figure 7. Comparison of speedline of the 2nd Configuration vs. Data Match of IGV + 2 Stage.

Figure 8 is a comparison of speedlines of configuration 1 & 2 vs. data match computed from the IGV leading edge to the Stator 1 trailing edge and shows that the configuration 2 results for stage 1 are consistent with that of configuration 1. Thus the addition of the second stage to the simulation is still missing the level of loss in stage 1.

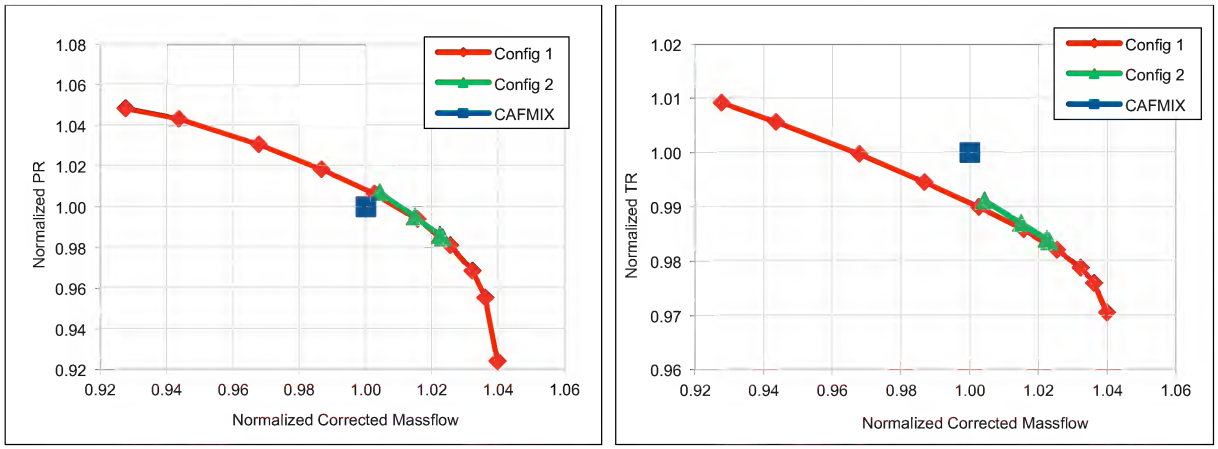

Figure 8. Comparison of Speedline of Configuration 1 & 2 vs. Data Match of IGV + 1 Stage.

Since the data match contained profile data, the total pressure and temperature downstream of Stator 1 from the numerical simulation were compared to the data match to see where the numerical simulations disagree with the data match. This comparison of profiles is shown in Figure 9. The normalized pressure ratio is measured from the IGV leading edge to Stator 1 trailing edge and is normalized by the integrated pressure ratio at the Stator 1 trailing edge from the CAFMIX solution. Similarly, the normalized temperature ratio is also measured from the IGV leading edge to Stator 1 trailing edge and is normalized by the integrated temperature ratio from the CAFMIX solution. The numerical solution from the Configuration 1 speedline is the solution closest in normalized corrected massflow which occurs at about 0.997 in Figure 6 and develops a normalized Pressure Ratio of 1.024. The numerical solution from the Configuration 2 speedline is the lowest normalized corrected massflow point which occurs at 1.005 and develops a normalized pressure ratio of 1.058. Note again that Configuration 1 is a single stage calculation and Configuration 2 is the two-stage geometry. It is apparent in Figure 9 that both numerical solutions develop a higher total pressure near the end walls than the data match but compare well near mid-span. As indicated earlier, the data match has a higher level of loss than the numerical simulations which may be from endwall blockage and results in a lower total pressure. The reason for this difference is not known at this time but certainly reinforces the need to investigate this experimentally. The total temperature profiles of the numerical simulations for both configurations match well with each other but underpredict the level of the data match. Again, the reason for this discrepancy is not known but will be investigated in the experiment.

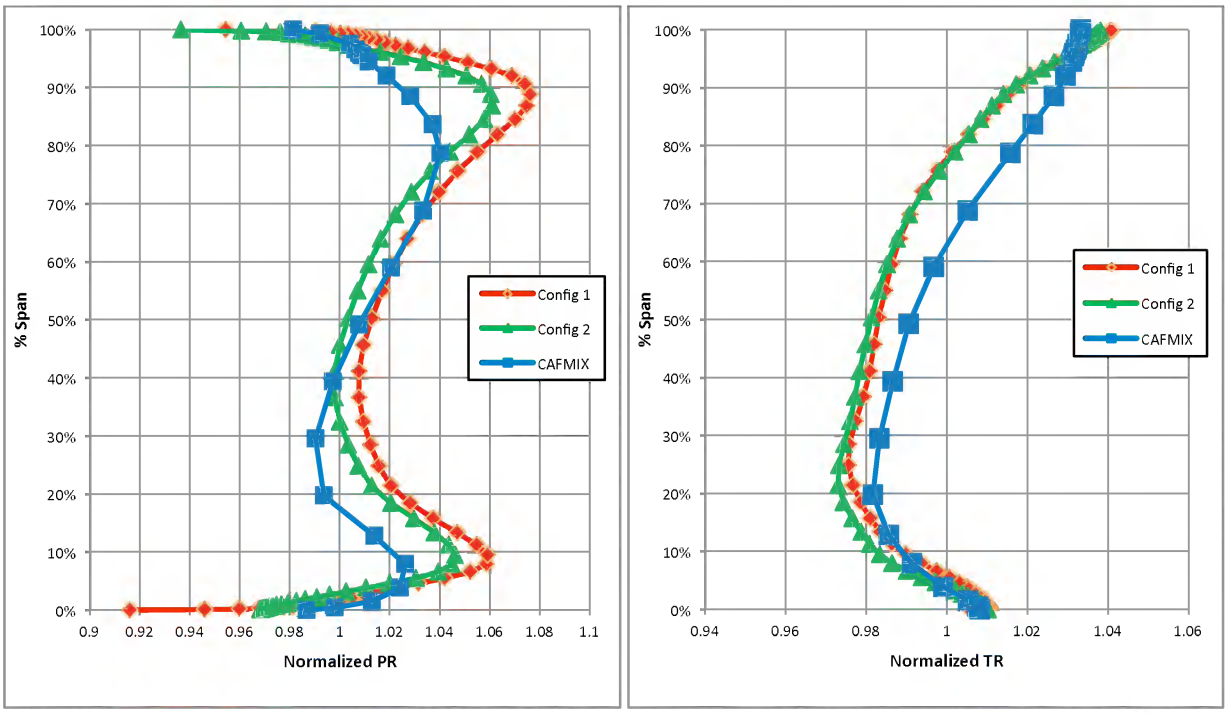

Figure 9. Comparison of Normalized Pressure and Temperature Ratio of both configurations vs. the Data Match at Stator 1 Trailing Edge.

Finally, the overprediction in total pressure and underprediction in total temperature can be shown in terms of a difference in adiabatic efficiency normalized by the data match. This, in essence, is a percent difference between the numerical solutions configurations 1 and 2, and the data match. The difference is about 6 percent for configuration 1 and about 5.5% for configuration 2 from the data match which is very large and underscores the need to understand what flow physics are being missed in the numerical simulations.

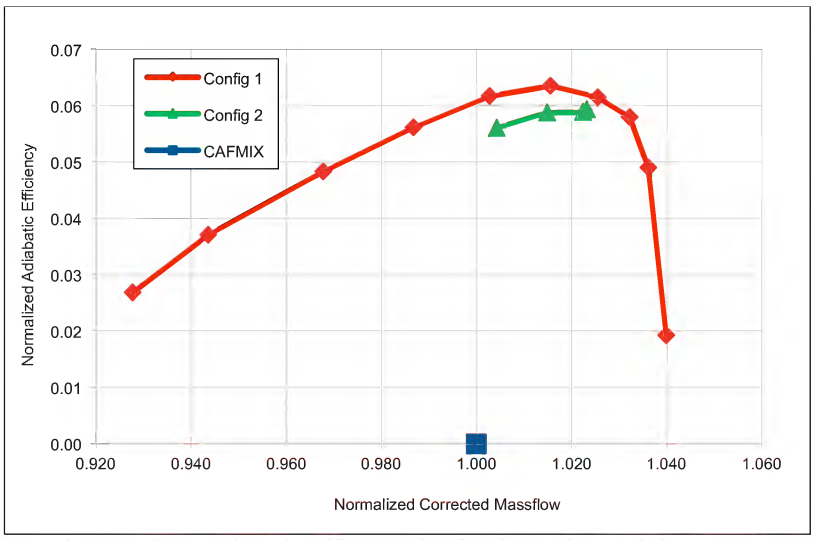

Figure 10. Comparison of Normalized Adiabatic Efficiency for Configurations 1 & 2 vs. Data Match at IGV + 1 Stage.

VII. Conclusion

An analysis code developed by NASA for multistage turbomachinery was used to simulate the first and second configuration of an advanced GE transonic compressor stage representing the front block of a core compressor. The first configuration is a single stage geometry and the second configuration is a two stage geometry. The objective was to generate a speedline of the stage at 97% Nc and compare those results to a data match solution before testing both configurations. The speedline overpredicted the total pressure and underpredicted the total temperature of the data match solution. Spanwise profiles were compared to the data match and showed that the end wall loss levels were underpredicted as well as level of total temperature. This resulted in about a 6% higher prediction of adiabatic efficiency and underscored the need to run this test.

Acknowledgments

This work is sponsored by the NASA Environmentally Responsible Aviation Project of the Integrated Systems Research Program. The authors wish to extend their sincerest thanks to Dr. Fay Collier, ERA Project Manager, Dr. Ken Suder, Propulsion Technology Sub-project Manager and the entire ERA Leadership team for their ERA project support and encouragement to promote the research discussed in this paper. The authors also wish to extend their thanks to Mr. Andy Breeze-Stringfellow, GE Aviation, in providing the CAFMIX solution and helpful discussions in this work.

References

[1]Adamczyk, J. J. "Model Equation for Simulating Flows in Multistage Turbomachinery." 1984. ASME Paper 85-GT-226 (NASA TM-86869).

[2]Adamczyk, J. J., Mulac, R. A. and Celestina, M. L. 1986. "A Model for Closing the Inviscid Form of the Average-Passage Equation System." ASME Paper 86-GT-227 (NASA TM-87199).

[3]Adamczyk, J. J., Celestina, M.L., Beach, T.A., Barnett, M., "Simulation of 3-D Viscous Flow Within a Multi-Stage Turbomachine." 1989. NASA TM-101376.

[4]Kirtley, K. R., Beach, T. A. and Adamczyk, J. J., "Numerical Analysis of Secondary Flow in a Two-Stage Turbine." 1990. AIAA-90-2356.

[5]VanZante, D., Strazisar, A., Wood, J., Hathaway, M., Okiishi T., "Recommendations for Achieving Accurate Numerical Simulation of Tip Clearance Flows in Transonic Compressor Rotors", Journal of Turbomachinery, October 2000, Vol. 122., P. 733.

[6]Shabbir, A., Zhu, J. and Celestina, M. L., "Assessment of Three Turbulence Models in a Compressor Rotor.", ASME 96-GT-198, 1996.

[7]Beach, Timothy. "A Grid Generation Procedure for Multiple Blade Row Axial and Radial Turbomachinery.", NASA CR-185167, 1991.

[8]Adamczyk, John J., Hansen, Jeffrey L and Prahst, Patricia S., "A Post Test Analysis Of A High-Speed Two-Stage Axial Flow Compressor.", ASME GT2007-28057, 2007.